M. KALLEK*, S. ATAOGLU**, Y. YAGCI*, H.N. BOZKURT *, A.N. GULLUOGLU***

IN THE JEWELRY, BRAZING AND LASER WELDING WITH PARAMETER OPTIMIZATION

OPTYMALIZACJA PARAMETRÓW LUTOWANIA I LASEROWEGO SPAWANIA JUBILERSKICH STOPÓW ZŁOTA

In this study, brazing and laser welding were experimentally compared for 9, 14 and 18 carat gold alloys in different color. The gold alloys were joined by laser welding and brazing and the microstructure, hardness, chemical composition, color of the weld joints were investigated. According to study, in laser welding, voltage, pulse duration, pulse diameter and frequency are the most important welding parameters that influence the quality of joints. Welded joints are characterized using three geometric parameters: penetration depth, width of heat affected zone and underfill defects. Finally, optimum laser welding parameters of different color of 9, 14 and 18 carat gold alloys were determined. It is observed that laser welding has numerous advantages compared to the other joining techniques used in the jewelry industry.

Keywords: laser welding, brazing, jewelry, gold alloys, carat

W pracy, porównano eksperymentalnie lutowanie i spawanie laserowe 9, 14 i 18 karatowych stopów złota o różnym kolorze. Zbadano mikrostrukturę, twardość, skład chemiczny i kolor połączeń. Wyniki badań spawania laserowego wskazują, że napięcie, czas trwania impulsu, średnica impulsu i częstotliwość to najważniejsze parametry, które wpływają na jakość połączeń. Spawane połączenia opisać można przy użyciu trzech geometrycznych parametrów: głębokość penetracji, szerokość strefy wpływu ciepła i defektów wypełnienia. Ustalono optymalne parametry spawania laserowego 9, 14 i 18 karatowych stopów złota o różnym kolorze. Stwierdzono, że spawanie laserowe ma wiele zalet w porównaniu do innych technik łączenia stosowanych w przemyśle jubilerskim.

1. Introduction

Gold and its alloys have been known for thousands of years, but their structures still are less known than, for example, the structures of other industrial materials. The composition and the technical know-how in making these alloys, either in the shape of gold jewelry or coins were secret for a long time. Many of gold alloys are based on traditional compositions and are still used extensively. Apart from jewelry manufacture, there are other areas where joining processes are widely used. Traditionally, brazing is the joining method used in jewelry manufacture. However, this method has several disadvantages, namely when high temperatures are achieved during cutting operations, giving rise to tips detachment. In such cases, a welding joint can be the best solution. In order to minimize residual stresses caused by the welding process, the joining method should minimize the heat affected zone (HAZ) and the heat input in the welding zone. Laser welding could be a good alternative, for joining gold and its alloys [1].

The application of laser welding in jewelry manufacture began about 20 years ago: now more than 3000 pulsed laser welders are used all over the world. Laser welding is a high energy density, focused laser light beam to apply energy to very small areas, resulting in very rapid, efficient local melting and low heat input, a process with specific advantages over other conventional welding processes. These include narrow HAZ, low distortion, ease of automation, minimal loss of material, to weld without filler materials, single-pass thick section capability and enhanced design flexibility. On the other hand, thermal diffusivity of the base material plays a large role: if the diffusivity is high, the material cooling rate is high and the HAZ is relatively small and the amount of heat inputted by the welding process also plays an important role since processes like oxy-fuel welding have a high heat input and increase the size of

*   GOLDAS JEWELRY INC., ISTANBUL, TURKEY

**   ISTANBUL TECHNICAL UNIVERSITY, CIVIL ENGINEERING DEPT., ISTANBUL, TURKEY

***   MARMARA UNIVERSITY, METALLURGICAL AND MATERIALS ENGINEERING DEPT., ISTANBUL, TURKEY

the HAZ. Processes like laser and electron beam welding give a highly concentrated, limited amount of heat, and result in a small HAZ [2, 3]. Laser welding has recently received growing attention due to its special features and potential. The advantages of increasing the power density of the heat source are deeper weld penetration, higher welding speeds, and better weld quality with less damage to the workpiece [4-6].

Laser welding is an important joining technique for many metals and their alloys (e.g. aluminum, magnesium, titanium, steel, nickel, shape memory alloys, bulk metallic glass etc.). Many laser welding parameters affect the welding quality: voltage, pulse duration, pulse diameter, frequency etc. are considered as the base laser welding parameters and should be optimized for high welding quality of gold alloys. Unsuitable welding parameters can result in many defects in gold and gold alloys. On the other hand, in order to achieve optimum welding in production laser welding quality and productivity should be optimized.

2. Experimental work

In this study, the brazing commonly used in the jewelry industry and laser welding are investigated for comparison of the joints. 9, 14, 18 carat (ct) gold alloys with different color are welded and brazed with systematically changed parameters and their effects on quality of the material were investigated on cross-sections. After that, braze metal and welded joint areas were investigated by metallographic and mechanical tests. These tests include: chemical composition analysis (XRF), phase composition analysis (SEM-EDS), hardness and color analysis on samples taken from laser welded and braze joint areas. Selected models of gold alloys joined by brazing and laser welding to determine joining time. Analysis of the results was aimed at developing optimum laser welding parameters for jewelry application.

The materials used in this study comprised 9, 14 and 18 ct gold alloy sheets in three color-yellow (ata), white and red. The sheets were cut into two small pieces for laser welding and brazing, each with sizes of $200 \times 200 \times 5mm^3$.

The gold alloys are made of Goldas Inc. in Turkey and their compositions are trade-secret. These alloys are made of using investment casting method whose details are available in Ref. [7].

In the brazing studies, microstructure and mechanical properties of base and braze metal were investigated. The specimens were cast by investment casting and sheets were heat treated at 750°C, 30 min. and then cooled in a furnace with 5°C/s cooling rate. Brazing of gold alloys in this study was carried out by the conventional method of inserting a sheet of the alloys indium alloys between the two parts to be joined and heating the sheet locally with an oxygen/hydrogen flame (oxygen volume is always half of hydrogen) by gas generator until it fused. The gas generator is a unit of system that does not require a separate external fuel source.

In brazing involves a filler metal composition that is different from the base metal composition and low melting temperature base metals must be added to produce braze sheets in the gold alloys. For this purpose, indium was added to the different color 9, 14, 18 ct gold alloys. After brazing, a boric acid-water-borax flux mixture was used to dissolve oxide residues on gold alloy sheet surfaces and the brazed alloys was then cleaned with sulphamic acid and dried under high pressure steam conditions.

Following the brazing, the microstructure, hardness and color of the base and braze metals were investigated and the relationship between microstructure, hardness, color and differences of base and braze metals were determined.

The brazed 9, 14 and 18 ct gold alloy cast sheets are shown in Fig. 1. As can be seen the high heat input and long brazing time also results in a poor surface smoothness. Due to its limited power density, the joining speed is very low and the total heat input per unit length of the joint is rather high, resulting in surface defects.
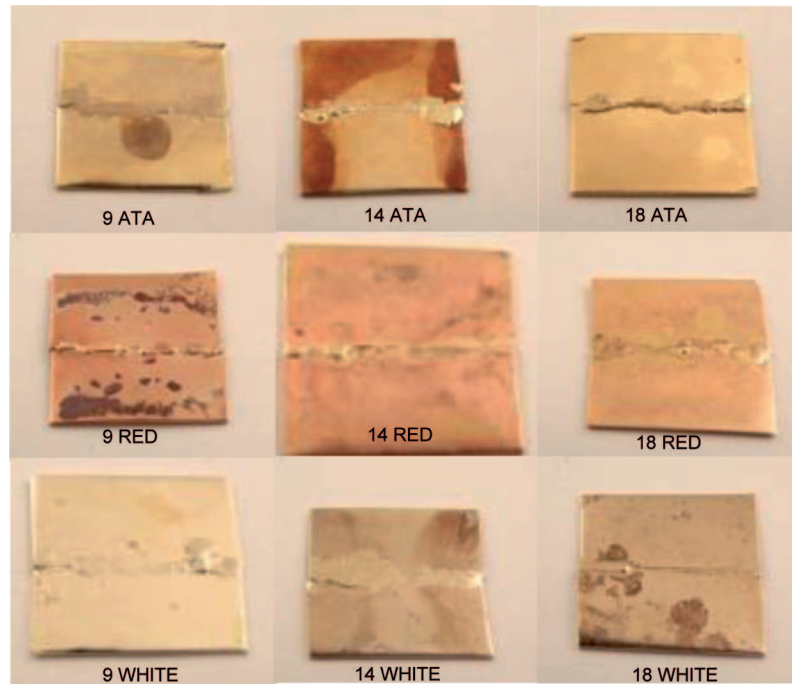
Fig. 1. Brazed gold alloy sheets

The laser welding process was performed using a LaserStar 7000 Series (Class 4) Nd:YAG laser at an average power of 60 W. The effects of the laser parameters (voltage, pulse diameter, pulse duration and frequency) were examined and compared to the parent alloys and brazing results by mechanical and metallographic tests.

Metallographic samples of the parent alloys, the brazed and laser welded joints were taken and prepared by standard polishing and etching techniques. The etching agents used were aqua regia (HCl: HNO_3 solution in volume ratio of 3:1) and cyanide-based (10 g potassium cyanide/100 ml water + 10 g Ammonium peroxidisulphate/100 ml water) solutions. Aqua regia is less useful for alloys with higher silver content and cyanide based etchants are the most versatile. Table 1 lists the etching agents for gold alloys used in this study.

The microstructure of the joints and parent alloys was characterized and the dimensions of the laser welds were measured using a Nikon Eclipse ME600 optical microscope. The chemical compositions of the gold alloys were determined by X-ray Fluorescence using Spectro MIDEX XRF equipment. Microstructure of the parent alloys and joints was characterized using Jeol, JSM-5910LV scanning electron microscope and Oxford INCA energy dispersion spectrometer.

The color analysis of gold alloys was determined by using a Minolta CM-508i color spectrophotometer by CIELAB method. The CIELAB method expresses color as 3-D coordinates: L, a, and b, where L is the luminance (brightness): L value of 0 means that no light is reflected by the sample and a L value of 100 means that all incident light is reflected. The a co-ordinate measures the intensity of the green (negative) or red (positive) component of the spectrum, while the b co-ordinate measures the intensity of the blue (negative) or yellow (positive) component.

TABLE 1

Used etching agents in gold alloys

Name	Etchant	Metals
Aqua Regia	60 ml Hydrochloric acid HCl + 20ml Nitric acid HNO_3	9 ct red, 14 ct ata, 14 ct red, 14 ct white 18 ct red, 18 ct white
Cyanide based etchant	10 g potassium cyanide KCN/100 ml water+ 10 g Ammonium peroxidisulphate, $(NH_4)_2S_2O_8$ /100 ml water	9 ct ata, 9 ct white, 18 ct ata

Hardness tests were performed on Struers Duramin-5 hardness tester. Results of hardness tests were evaluated by averaging the results of three measurements. The hardness measurements were done at the parent metal surface and laser weld and braze joint. Vickers hardness (HV1) measurements (1 kg load, applied for 5 s) were performed at room temperature.

The influence of the basic parameters of laser welding on shape and quality of the joints and the range of optimal parameters of welding were determined. The geometry of the welded cross-section gives very important information about the quality of the laser welding. The welded cross-sections of the materials are characterized by using three geometric parameters. The first one, "H1" represents penetration depth. Laser welding application begins with the determination of parameters for optimal conditions which is the most important parameter affected on penetration depth (H1). The second, "H2" represents the width of the HAZ, whilst the third, "H3" represents the dimensions of underfill defects. Highly focused energy is transferred by means of laser beam during the welding and this energy melts the material without vaporization. If the transferred energy is higher, the material loss comes up in weld pool and it is indicated as a crater formation with the depth of "H3". These distances are shown schematically in Fig. 2.
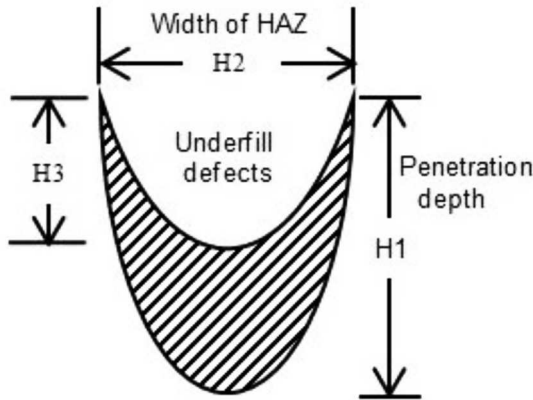

Fig. 2. Characterization of laser welded cross-sections

3. Results and conclusions

3.1. Brazing

Firstly, joining times of the 9, 14 and 18 ct gold alloys were measured. As is seen in Fig. 3, the average joining time is about 83 s for two specimens of each gold alloys.

After brazing, nine different compositions of brazed gold alloys have been analyzed. Cross-sectional samples for metallurgical examination were cut from the braze joints. Six of all samples were etched with aqua regia and the others were etched with the cyanide-based solution to reveal details of the microstructure, which was examined by an optical microscope. The microstructures are presented in Fig. 4. As can be seen, the parent metal/braze joint boundary is not very distinct. The microstructure of parent metal and braze area different but dendritic structures were detected in both microstructures. The parent and braze metal microstructure had a different color and composition. Strong segregation was revealed and small interdendritic shrinkage pores are present in the as cast structure. The heat input involved in brazing is very high; the joint quality can be rather poor.

Table 2 gives the CIELAB color co-ordinates for the gold alloys examined. The L values were high in all the samples and not affected much by the alloying additions. The addition of indium in braze markedly decreased a and b values for the yellow color gold alloys especially, making them darker. The addition of a small amount of indium and the effect of the high heat input to the red and white alloys appreciably decreased both a and b values. As a result, braze and parent metal color values are different and this undesirable.

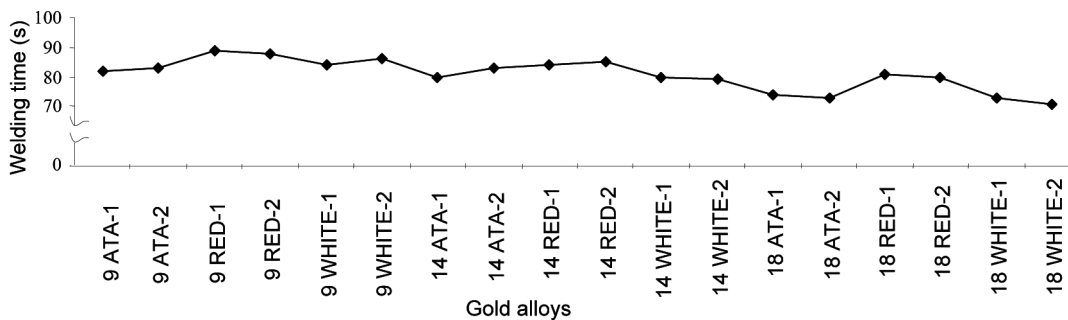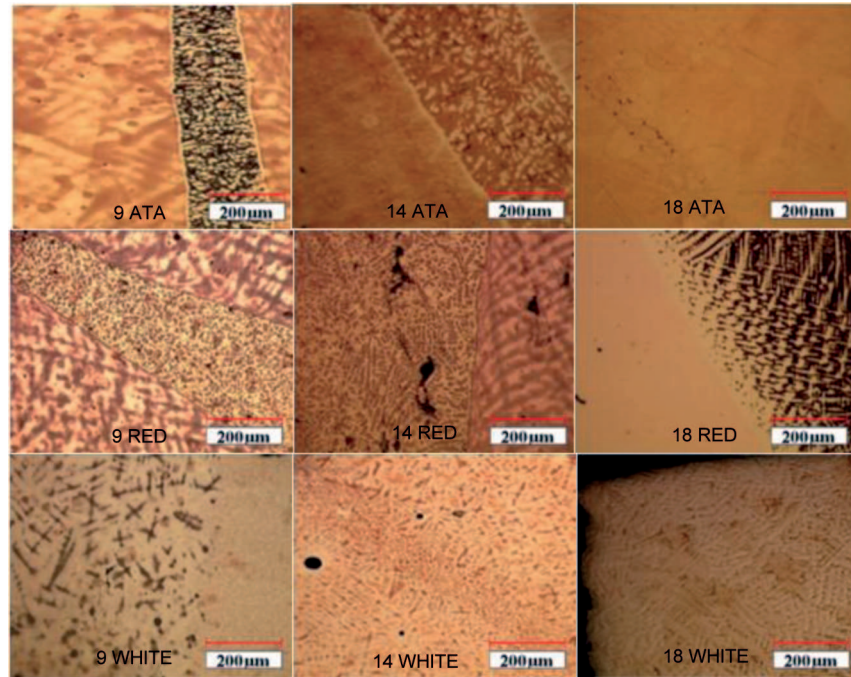

Fig. 3. Brazing time of gold alloys

Fig. 4. Microstructure of base metal/weld joints of gold alloys

TABLE 2

Color analysis of braze and base metal

Element	Values		
	L	a	b
9 ct ata base metal/brazed area	87.82/90	0.78/-1.08	26.68/15.06
9 ct red base metal/brazed area	82.9/85.81	14.11/4.58	19.24/19.43
9 ct white base metal/brazed area	84.54/85.5	0.37/0.22	10.62/11.75
14 ct ata base metal/brazed area	88.65/90.45	1.14/-1.39	27.34/20.4
14 ct red base metal/brazed area	79.4/86.3	13.21/6.83	19.63/17.57
14 ct white base metal/brazed area	83.1/84.5	1.86/0.55	16.74/15.68
18 ct ata base metal/brazed area	88.65/88.54	1.14/1.37	27.34/24.79
18 ct red base metal/brazed area	84.23/86.3	9.23/6.83	24.67/17.57
18 ct white base metal/brazed area	85.04/87.35	1.84/0.94	18.91/18.75

The average hardness from at least three indentation tests is shown in Fig. 5. For gold alloys, there is an increase in hardness of the brazed metal compared to the parent metal. For example, the average hardness in the 9 ct white gold alloy is approximately 211 HV1 as compared with a hardness of 193 HV1 in the parent metal. This increase was probably due to a higher volume fraction of intermetallic phases due to the indium.

Figs. 6-7 show SEM-EDS analysis of 14 ct red and 18 ct white gold alloys after brazing, showing that small interdendritic shrinkage pores and microstructures different from the parent metal, because that higher volume fraction of intermetallics containing indium. Details of the other gold alloys are available in Ref. [7]. The final microstructure and mechanical properties of braze and HAZ will depend on the heating and cooling rates. In brazing, high heat inputs to the workpieces, results in lower cooling rates and the grain structures are coarser.
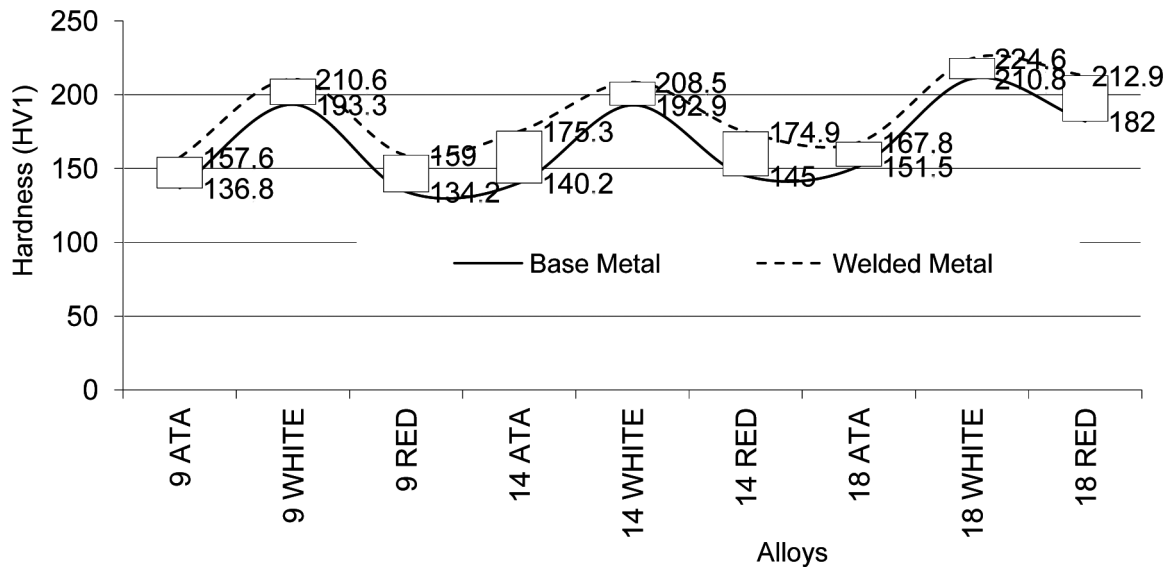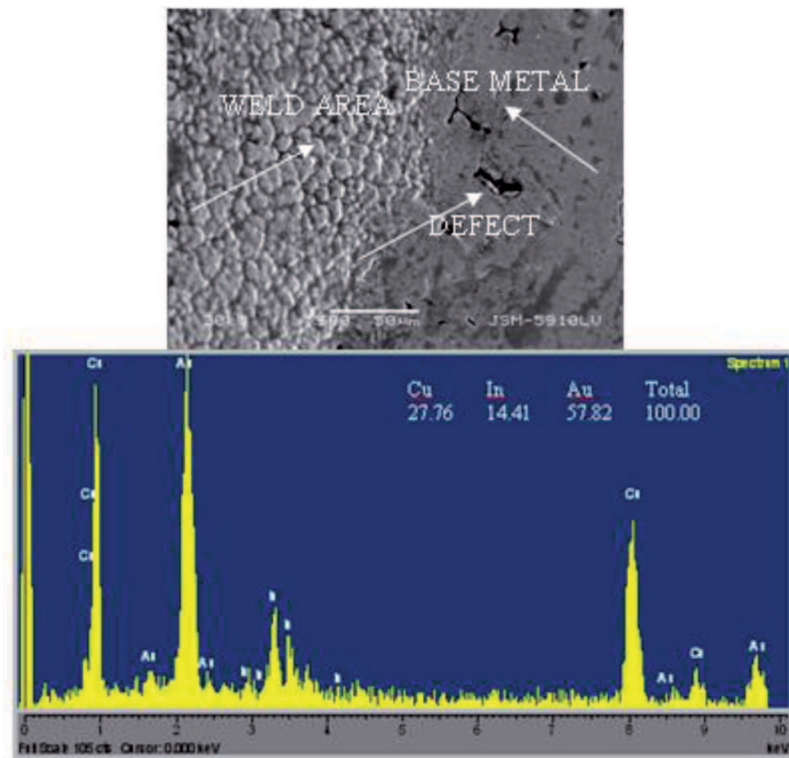
Fig. 5. Brazing hardness values

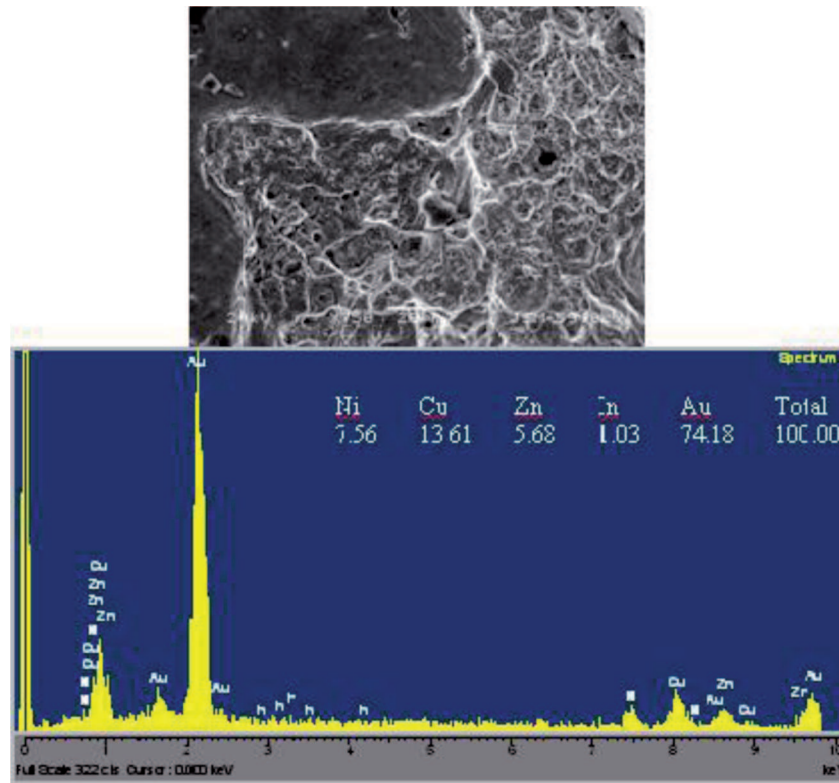Fig. 6. 14 ct red gold alloy brazing SEM-EDS results

Fig. 7. 18 ct white gold alloy brazing SEM-EDS results

3.2. Laser welding

Measured laser welding times of the 9, 14 and 18 ct gold alloys gave an average welding time of about 59 s for two specimens of each gold alloys (Fig. 8). The time of laser welding is extremely short (24 s) as compared with brazing. High thermal conductivity materials like aluminum, copper and gold are difficult to weld because the surface absorptivity of these materials decreases as their conductivity increases. Reflectivity depends on both inherent optical properties of the materials (e.g., absorption coefficient for certain wavelength radiations) and specularity (i.e., smoothness or polish). As seen in

Fig. 8, welding times of the red gold alloys are much longer than for white and yellow gold alloys, because of the high reflectivity of red gold alloys.

Chemical analysis of the laser welds and parent metal, Table 3 shows that they are similar, as might be anticipated. As seen in Table 3, zinc evaporates from molten metal due to low vapor pressure so that lower zinc content of the weld than parent alloys.

Table 4 gives the CIELAB color co-ordinates for the welded gold alloys examined. In the contrary braze color analysis result. The L, a and b values of parent metals are similar laser weld joints.
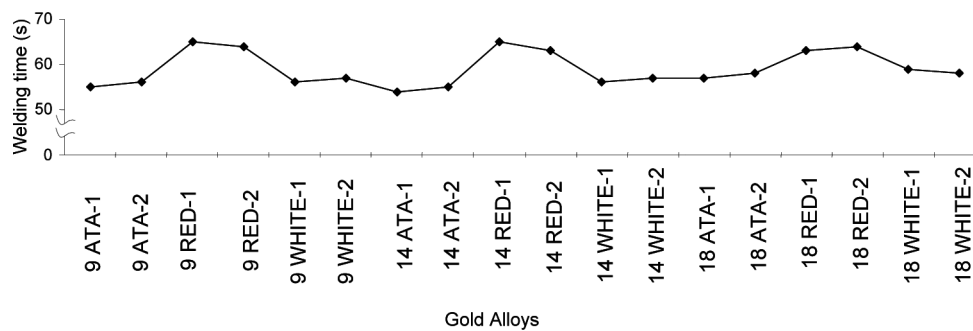

Fig. 8. Laser welding time of gold alloys

TABLE 3

Chemical composition of laser weld and base metal

		9 ct			14 ct			18 ct		
	Element	Ata	White	Red	Ata	White	Red	Ata	White	Red
Base metal XRF analysis	Au	37.64	37.75	37.58	58.78	58.69	59.15	75.69	75.41	75.85
	Cu	29.88	9.39	62.42	23.15	19.02	40.85	12.36	14.49	18.87
	Zn	14.16	4.35	-	9.95	3.45	-	-	6.42	3.89
	Ag	17.32	48.51	-	8.12	8.15	-	11.95	-	1.39
	Ni	-	-	-	-	10.69	-	-	3.68	-
	Si	1.00	-	-	-	-	-	-	-	-
	In	-	-	-	-	-	-	-	-	-
	Total	100.00	100.00	100.00	100.00	100.00	100.00	100.00	100.00	100.00

		9 ct			14 ct			18 ct		
	Element	Ata	White	Red	Ata	White	Red	Ata	White	Red
Weld metal XRF analysis	Au	37.65	38.21	37.85	58.69	58.77	58.80	75.69	75.59	75.90
	Cu	28.46	11.25	62.15	22.56	18.46	41.20	11.56	14.00	18.43
	Zn	14.00	4.15	-	9.48	4.68	-	-	6.15	3.85
	Ag	19.04	43.02	-	9.27	5.30	-	12.75	-	1.82
	Ni	-	3.37	-	-	12.79	-	-	4.26	-
	Si	0.85	-	-	-	-	-	-	-	-
	In	-	-	-	-	-	-	-	-	-
	Total	100.00	100.00	100.00	100.00	100.00	100.00	100.00	100.00	100.00

TABLE 4

Color analysis of laser weld and base metal

Materials	Illuminant D65			Illuminant F11		
	L	a	b	L	a	b
9 ct ata base metal	87.82	0.78	26.68	89.13	1.11	30.07
9 ct ata laser welded area	89.06	0.94	27.32	90.43	1.31	30.77
9 ct red base metal	82.90	14.11	19.24	83.50	15.34	22.63
9 ct red laser welded area	80.87	13.89	19.78	84.11	14.94	21.41
9 ct white base metal	84.54	0.37	10.62	83.02	0.83	11.93
9 ct white laser welded area	83.08	0.19	10.80	83.58	0.69	12.16
14 ct ata base metal	88.65	1.14	27.34	89.99	1.54	30.76
14 ct ata laser welded area	87.94	1.34	28.46	89.35	1.71	34.02
14 ct red base metal	78.95	14.58	21.74	80.25	15.28	24.70
14 ct red laser welded area	79.40	13.21	19.63	80.89	14.04	22.42
14 ct white base metal	83.10	1.86	16.74	83.83	2.15	18.82
14 ct white laser welded area	83.04	1.86	16.69	83.91	2.14	18.79
18 ct ata base metal	88.65	1.14	27.34	89.99	1.54	30.76
18 ct ata laser welded area	87.94	1.34	28.46	89.35	1.71	34.02
18 ct red base metal	84.23	9.23	24.67	85.97	8.70	28.05
18 ct red laser welded area	85.50	9.23	24.00	87.05	8.65	27.24
18 ct white base metal	83.62	2.21	20.47	84.71	2.61	23.19
18 ct white laser welded area	85.04	1.84	18.91	86.03	2.22	21.37

The hardness test has been carried out optimum welds of eight specimens of each of the nine gold alloys; the average hardness of each gold alloy is listed in Fig. 9. As a result, at the center of the weld pool, the hardness is at the maximum level and the melted and cooled material is remarkable compared to the parent metal due to its rapid cooling rate. For example, as can be seen in Fig. 9 for the 18 ct white gold alloy, the difference in hardness between the weld pool and the parent metal is 53 HV. In the HAZ, heating arises from the weld pool so the hardness is lower than the weld pool and the difference is 40 HV. The difference between the HAZ and the parent metal is 11 HV. The average hardness of the weld pool of gold alloys was higher than that of the parent metal. This was due to the fine grain structure of the weld pool. The HAZ of the gold alloys was relatively small due to the low energy input and short welding time. As a general rule, an attempt is made to design the weld to be stronger than the base materials. High power density of laser welding provides a lower heat input and a more rapid solidification when compared to brazing, so laser welding technique leads to higher hardness values.

3.3. Determination of optimum laser welding parameters

The optimum laser parameters were investigated for 9, 14 and 18 ct gold alloys. Only three specimens are presented in this work but the others can be found in Ref. [7]. The frequency was 2 Hz for all specimens. The laser peak power was 60 W and gas pressure 2 bar.

The effects of laser welding parameters on geometric distances for the 9 ct yellow gold cast sheets are shown in Table 5. Fig. 10a shows the optical micrographs at workpiece 1, voltage of 225 V, pulse duration of 3 ms, and pulse diameter 1 J/m^2. As can be seen, welding has not occurred. Fig. 10b-c shows optical and scanning electron micrographs of the cross-sections of workpieces 5 and 6 welded under the pulse diameter from 1 to 1.5 J/m^2 to understand the effect of pulse diameter. The voltage and pulse duration has been kept constant 300 V and 3 ms. As can be seen, H2 value increased with increase of pulse diameter at constant voltage and pulse duration. Unsuccessful results can be obtained if the underfill defects (H3) are too large if significant vaporization occurs during welding. To overcome this defect and make the best weld, the voltage has been decreased (Fig. 10d-e). The best weld was obtained (Fig. 10e) when voltage, pulse duration and pulse diameter are 250 V, 3 ms and 1.5 J/m^2, respectively with geometric distances of H1=246.65 μ, H2=516.67 μ and H3=0, which do not be seen underfill defects (H3) on weld area.

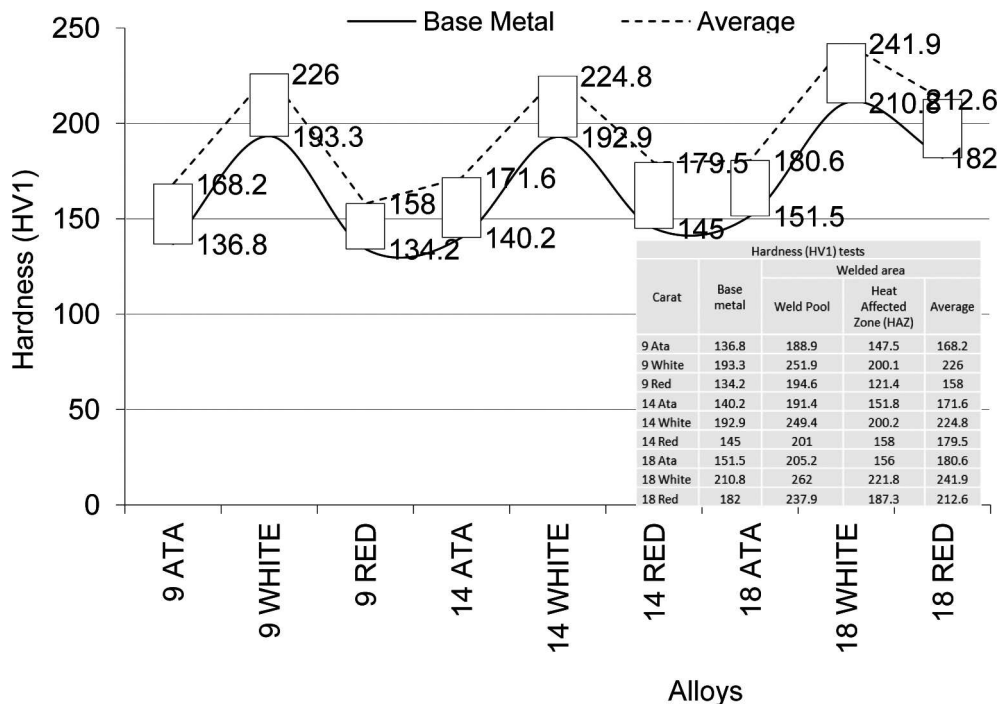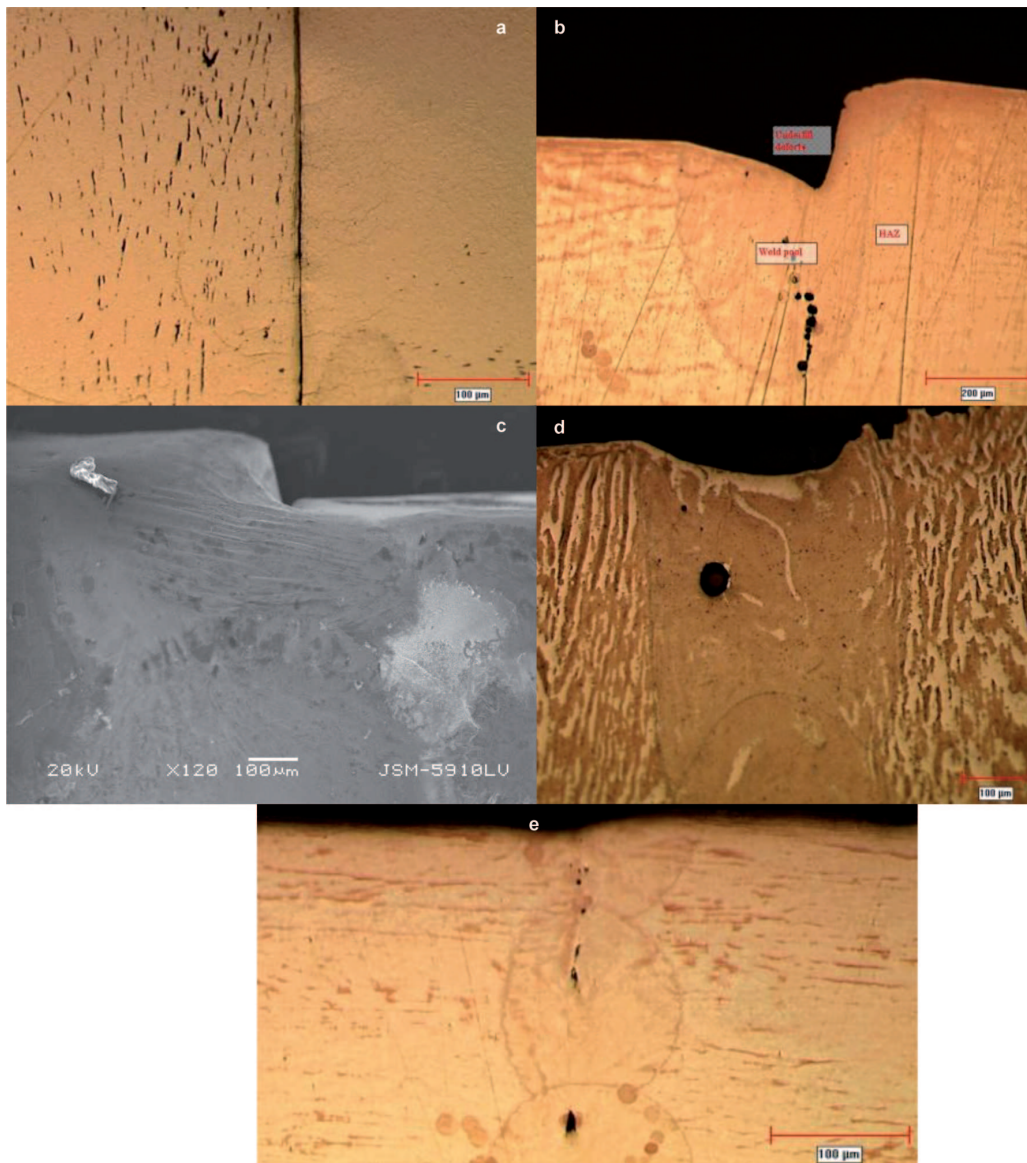| Hardness (HV1) tests				
		Welded area		
Carat	Base metal	Weld Pool	Heat Affected Zone (HAZ)	Average
9 Ata	136.8	188.9	147.5	168.2
9 White	193.3	251.9	200.1	226
9 Red	134.2	194.6	121.4	158
14 Ata	140.2	191.4	151.8	171.6
14 White	192.9	249.4	200.2	224.8
14 Red	145	201	158	179.5
18 Ata	151.5	205.2	156	180.6
18 White	210.8	262	221.8	241.9
18 Red	182	237.9	187.3	212.6

Fig. 9. Laser welding hardness values

Fig. 10. 9 ct ata micrographs: a) workpiece 1 b) workpiece 5 c) workpiece 6 d) workpiece 3 e) workpiece 2

The effect of 9 ct ata welding parameters on geometric distances

No	H1 (μm)	H2 (μm)	H3 (μm)	Voltage (V)	Pulse diameter (J/m^2)	Pulse duration (ms)
1	-	-	-	225	1	3
2	246.65	516.67	0	250	1.5	3
3	309	335	54.01	275	1	5
4	316	717	86.3	275	1.5	5
5	530.55	360.26	156.73	300	1	3
6	524.6	695	150	300	1.5	3
7	-	-	-	325	1.5	5
8	-	-	-	325	1.5	8

As seen in Table 6, the high voltage results in high vaporization for the 14 ct red gold alloy. The depth of underfill (H3) has the greatest value. As illustrated in Fig. 11a, welding was not occurred. Fig. 11b-c shows scanning electron and optical micrographs of the cross-sections of the workpieces 5 and 6 welded under the pulse duration from 3 to 5 ms, with pulse diameter and voltage kept constant to understand the effect of pulse duration. As seen in Fig. 11b-c the depth of penetration and underfill defects increased as pulse duration increased from 3 to 5 ms. Optimum welding condition of 14 ct red gold alloys is obtained, Fig. 11d with V=300 V, pulse duration=3 ms, pulse diameter=1 J/m^2 and geometric distances of H1=261.85 μ, H2=212 μ and H3=20.5 μ. Red gold alloys were welded at a higher voltage than white and yellow gold alloys; this situation can be explained by the high reflectivity of red gold alloys.

Table 7 shows 14 ct white alloy laser welding parameters. As can be seen Fig. 12a-b (workpieces 2 and 1)

the depth of penetration increases as voltage increased while the pulse duration and pulse diameter are fixed. The best weld was obtained, Fig. 12b, when voltage, pulse duration and pulse diameter were 250 V, 5 ms and 1.5 J/m^2, respectively. At higher voltages, it has been found that the width of the HAZ has increased with the voltage. In this case, due to longer interaction time between the laser pulse and the workpieces, wider weld pool and HAZ have been obtained. In Fig. 12 c-d it is seen that there is porosity during the welding process. This is due to the trapping of the some gas within the solidifying weld pool. During laser welding process formation and solidification of the melted material, hydrodynamic movements in the melted material (vortex formations) are the factors affecting size and dispersion of porosity. Pulse duration and voltage have been increased in order to obtain deeper penetration without any loss on the surface.
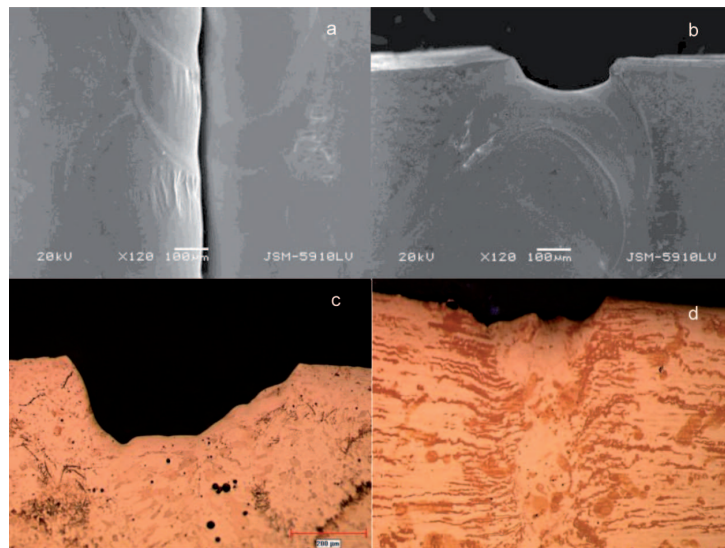

Fig. 11. 14 ct red micrographs: a) workpiece 2 b) workpiece 5 c) workpiece 6 d) workpiece 3

TABLE 6

The effect of 14 ct red welding parameters on geometric distances

No	H1 (μm)	H2 (μm)	H3 (μm)	Voltage (V)	Pulse diameter (J/m^2)	Pulse duration (ms)
1	-	-	-	250	1	3
2	-	-	-	275	1	3
3	261.85	212	20.5	300	**1**	3
4	298	426.75	61.91	300	1.5	3
5	420	617	108	325	1.5	3
6	524.6	608.98	199.12	325	1.5	5
7	-	-	-	350	1	3
8	-	-	-	350	1.5	3

The effect of 14 ct white welding parameters on geometric distances

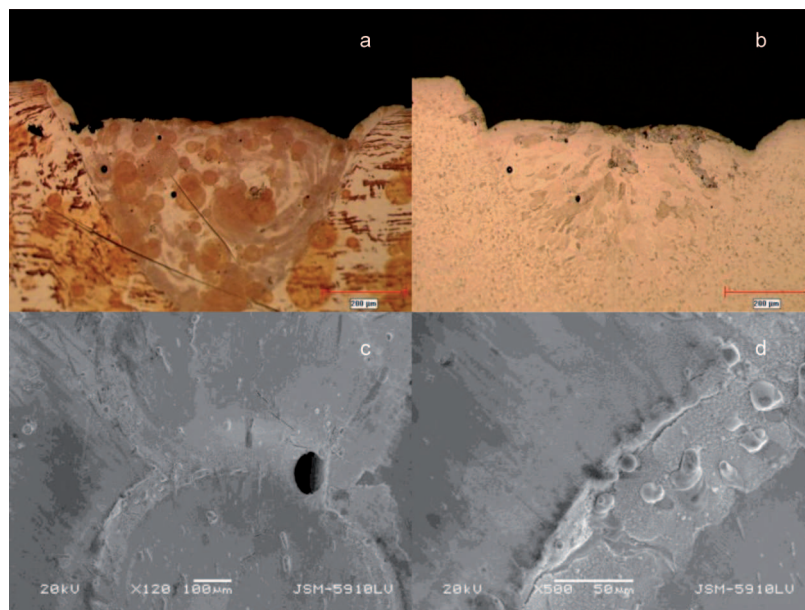| No	H1 (μm)	H2 (μm)	H3 (μm)	Voltage (V)	Pulse diameter (J/m^2)	Pulse duration (ms)
1	363.75	520.51	35.8	250	1.5	5
2	468.89	615.13	69.38	275	1.5	5
3	274.43	240.13	70.84	275	1	3
4	420.52	451.26	170	300	1.5	3
5	399.5	818	235	300	1.5	5
6	495	547.51	216	325	1	5
7	-	-	-	350	1	3
8	-	-	-	350	1.5	3

Fig. 12. 14 ct white micrographs: a) workpiece 2 b) workpiece 1 c) workpiece 6 d) workpiece 3

The results of this work can be summarized as:

- The time required for laser welding is extremely short (24 s) as compared with soldering/brazing.
- Because of the rapid cooling, the hardness of the laser welded zone is very high as compared to the parent metal. In soldering/brazing, compared to the base metal, the increase in hardness of the brazed area was probably due to the higher volume fraction of intermetallics includes due to the indium content.
- Brazed area color values are quite different compared to the parent metals, because of the difference in composition due to the indium content of braze. In contrast laser weld and parent metal areas were similar in color.
- The chemical composition of weld and parent metal are similar, but braze area were different of base metal because of using filler metal with indium. In fact laser welds have the overall advantage of producing, minimum HAZ, minimizing residual stresses and distortion.
- When compared to yellow and white gold alloys, red gold alloys were welded at higher voltages. This situation can be explained by the high reflectivity of red gold alloys.
- Compared to brazing, the cooling rate in laser welding is higher and the weld metal microstructure is finer.

The geometry of the welded cross-section gives very important information about the quality of the laser welding:

* Depth of penetration (H1) increases as voltage is increased at a fixed pulse duration and pulse diameter.

* To increase the penetration depth (H1) without craters (H3), pulse duration is increased at constant voltage.

* Weld width (H2) is increased with an increase in pulse diameter at constant voltage and pulse duration.

* If the voltage is increased too much underfill defects and HAZ increased, which promotes this situation, the voltage has been decreased the other parameters kept constant or the pulse duration has been increased at constant voltage.

* The HAZ for the laser welded sample was also much smaller than braze area. The low heat input and short welding time also ensures that there are insignificant losses of precious metals. The other advantages of laser welding include; low contamination risk, lowest porosity in the weld pool, easy of automation, deeper weld penetration, better weld quality and less damage to the workpiece.

REFERENCES

[1] M. G r i m w a d e, Handbook on Soldering and Other Joining Techniques, World Gold Council, London (2002).

[2] S. K o u, Welding Metallurgy, Wiley, New York (2003).

[3] W. K o e c h n e r, Solid-State Laser Engineering, Springer, Berlin (1999).

[4] L.K. P a n, C.C. W a n g, Y.C. H s i a o, K.C. H o, Optimization of Nd: Yag laser welding onto magnesium alloy via taguchi analysis, Opt. Laser. Technol. **37**, 33-42 (2005).

[5] Y.G. S o n g, W.S. L i, L. L i, Y.F. Z h e n g, The influence of laser welding parameters on the microstructure and mechanical property of the as-jointed NiTi alloy wires, Mater. Lett. **62**, 2325-2328 (2008).

[6] F.M. G h a i n i, M.J. H a m e d i, M.J. T o r k a m a n y, J. S a b b a g h z a d e h, Weld metal microstructural characteristics in pulsed Nd: Yag laser welding, Scripta Mater. **56**, 955-958 (2007).

[7] M. K a l l e k, Brazing and soldering in the jewellery industry using laser technology, Master Thesis, Marmara University, Istanbul (2009).